Article

Voltammetric Determination of Sophoridine Based on Gold Nanoparticles/L-cysteine/ Graphene Modified Glassy Carbon Electrode

Fei Wang,* Longtao Zhao, Liu Yang, Bei Li, Liming Qiang and Lin Gao
School of Material and Chemistry Engineering, Henan Institute of Engineering, Zhengzhou 450007, P.R. China

A new strategy to make the electrochemical sensor was presented, through combining gold nanoparticles (GNPs) with reduced graphene oxide (rGO) via L-cysteine (L-cys) as crosslinker. The resulting electrodes were characterized by scanning electron microscopy (SEM) and electrochemical methods. And it was applied to develop a high-sensitive electrochemical sensor for determination of sophoridine. Compared with the bare GCE and reduced graphene oxide modified electrode, the resulting electrodes exhibited excellent response toward the oxidation of sophoridine by significantly enhancing the oxidation peak currents and decreasing the overpotential of sophoridine. Under the selected conditions, there exist the linear relation between the oxidation peak currents and sophoridine concentration in the range of $1.0 \times 10^{-6} \sim 1.0 \times 10^{-4}$ mol L^{-1}, with detection limit of 4.0×10^{-7} mol L^{-1}. At the same time, the method can be successfully applied to the quantitative determination of sophoridine in injection samples and its result is satisfactory.

Keywords: Graphene; Gold nanoparticles; L-cysteine; Voltammetric sensor; Sophoridin.

INTRODUCTION

Sophoridine, a quinolizidine alkaloid, is a main active ingredient of kinds of *sophora plants* in traditional Chinese herbal drug.[1] The studies of pharmacological effect have shown that sophoridine has wide pharmacological effects including anti-inflammatory,[2-5] antitumor,[6,7] and antivirus.[8,9] At present, it has been extensively used to treat tumors, fever, throat inflammation, acute or chronic gastroenteritis. Accordingly, accurate analytical method for sophoridine is necessary. Some detection techniques have been developed, such as high performance liquid chromatography (HPLC),[10,11] gas chromatography-mass spectrometer (GC-MS),[12] capillary electrophoresis (CE),[13] chemiluminescence (ECL)[14] and electrochemistry.[15,16] Among these, electrochemical analysis has attracted more and more attentions due to the advantages of simplicity, easy miniaturization, high sensitivity, relatively low cost and excellent selectivity.

To achieve the determination, several forms of nano materials (e.g. ordered mesoporous carbon,[17] carbon nanotube[18] and gold nanoparticles (GNPs)[19]) have been studied to use for developing electrochemical sensors in the past decades. Graphene, a perfect two-dimensional carbon material found in 2004,[20,21] is an ideal material for electrochemistry[22] because of its very large 2D electrical conductivity, large surface area and low cost. On the other hand, GNPs also have been widely employed as a modifier in voltammetry for analysis of various species,[23,24] because of their large aspect ratio (surface area to volume), biocompatibility and high electrical conductivity.

In this work, we tried fabricating a new electrochemical sensor through combining gold nanoparticles (GNPs) with reduced graphene oxide (rGO) via L-cysteine (L-cys). The resulting electrodes were characterized by scanning electron microscopy (SEM) and electrochemical methods. And it was applied to develop a high-sensitive electrochemical sensor for determination of sophoridine using differential pulse adsorptive stripping voltammetry (DPASV). Electrochemical behaviors of sophoridine at the modified electrode were investigated by cyclic voltammetry (CV) and chronocoulometry (CC). At the same time, the method can be successfully applied to the quantitative determination of sophoridine in injection samples and its result is satisfactory.

EXPERIMENTAL

Apparatus and reagents: Model CHI 650A electrochemical system (CHI Instrumental, Shanghai, China) and RST5000 electrochemical workstation (Zhengzhou Shiruisi Instrument Co., Ltd., Zhengzhou, China) were employed for electrochemical techniques. Atomic Force Microscopy (AFM) images were obtained with a BenYuan CSPM-5500 atomic force microscopy (Guangzhou BenYuan nanometer Instrument Co., Ltd., Guangzhou, China). Transmission electron microscope (TEM) (Tecnai

---

* Corresponding author. Tel: +86 0371 67718925; Fax: +86 0371 67718909; Email: wf2003@haue.edu.cn

G²20 S-TWIN, FEI Company, Holland) was employed to observe the morphology. SEM images were obtained with a Quanta 250 scanning electron microscope (FEI Company, Czech). A standard three-electrode electrochemical cell was used with GCE (d = 3 mm) or modified GCE as a working electrode, platinum (Pt) wire as an auxiliary electrode and a saturated calomel electrode (SCE) as a reference electrode (the internal solution was saturated KCl solution). All the pH measurements were made with a PHS-3C precision pH meter (Leici Devices Factory of Shanghai, China), which was calibrated with standard buffer solution at 25 ± 0.1 °C every day. Sophoridine was purchased from National Institute for the Control of Pharmaceutical and Biological Products (Beijing, China). Stock solution (2.0×10^{-3} mol L^{-1}) of sophoridine was prepared with doubly distilled water and stored at 4 °C in the dark. Sophoridine hydrochloride injection was purchased from Tonghua fangda Pharma. Co., Ltd (Jilin, China). $HAuCl_4$ was obtained from Xiya reagent (Sichuan, China). GNPs were prepared as previously reported.[25] All reagents were of analytical grade and were used as received. Double distilled water was used for all preparations.

Preparation of the graphene oxide: Firstly, graphene oxide (GO) was synthesized from graphite by the modified Hummers method.[26] The exfoliated GO was obtained from the GO dispersion, which was under ultrasound and centrifugated at 4000 rpm for 15 min. The resulting GO deposited on the mica were characterized by AFM. The results found that the GO sheets were almost single-layer, seen in Fig. 1. And the average thickness of single-layer GO sheets was approximately 1 nm. The reduction of graphene oxide (rGO) using ascorbic acid was performed in water at room temperature for 24 h. In a typical experiment, 100 mg of ascorbic acid was added into 50 mL (0.1 mg mL^{-1}) of an aqueous dispersion of the graphene oxide under vigorous stirring. A powder of rGO was obtained by filtration and drying in air. The rGO was dispersed in N,N-dimethylformamide (DMF) at a concentra-
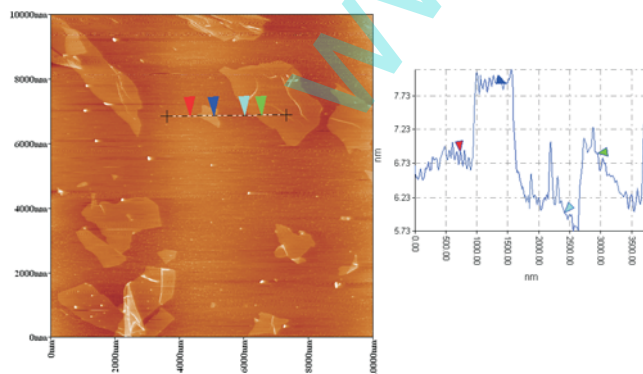
tion of 0.2 mg mL^{-1}, and the suspensions were stable at room temperature for about 3 weeks. Fig. 2 shows the TEM image of the wrinkled graphene with no aggregation.

Preparation of the modified electrode: Prior to modification, the bare GCE was polished successively with 0.3 and 0.05 μm Al_2O_3 power and rinsed thoroughly with doubly distilled water between each polishing step. After that, the GCE was sonicated in ethanol and doubly distilled water each for 2 min, and dried under N_2 blowing. After that, the bare GCE was inverted upside and 5 μL rGO solutions was dropped on the electrode surface with the micropipette. It was allowed to dry at room temperature. This modified electrode was named rGO/GCE. Then, the rGO/GCE underwent cyclic scanning between 0.0 V and 1.0 V in a phosphate buffer (0.5 mol L^{-1}, pH 7.0) until a stable voltammogram was attained. The rGO/GCE was next modified through sequential scanning within a potential range between -1.5 V and +2.4 V for three cycles in an L-cysteine solution of 0.1 mol L^{-1} concentration. The L-cysteine modified electrode (L-cys/rGO/GCE) was then rinsed with double-distilled water, followed by immersing in gold nanoparticles colloidal solution for 6 h under 4 °C to acquire the modified GCE of GNPs, named as GNPs/L-cys/rGO/GCE. The scheme 1 showed the schematic diagram for preparation of GNPs/L-cys/rGO/GCE.

Experimental procedure for electrochemical analysis: A certain volume of stock solution of sophoridine and 10 mL 0.2 mol L^{-1} pH = 7.5 phosphate buffer solutions (PBS) were added into an electrochemical cell, and then the electrode was immersed into the cell. The cyclic voltammetry (CV), chronocoulometry (CC) or differential pulse voltammetry (DPV) were performed to
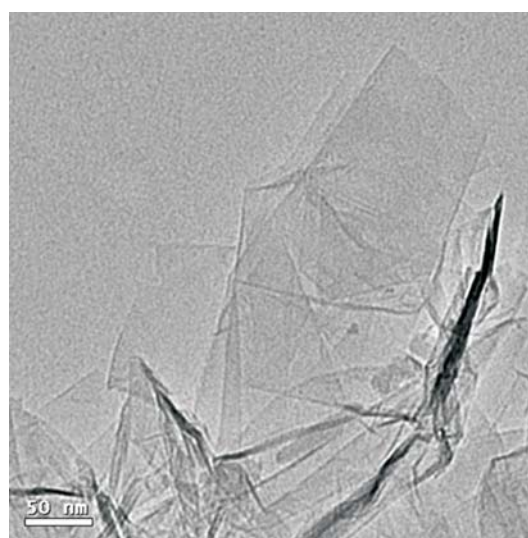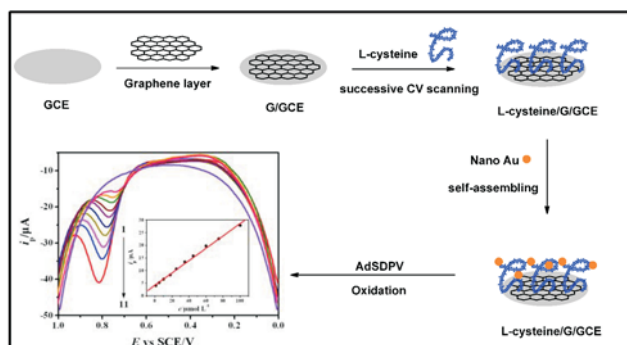

Fig. 1. AFM image of GO from its dilute aqueous dispersion on freshly cleaned mica.

Fig. 2. TEM image of rGO (acceleration voltage: 200 KV, metallization of the surface: copper).

investigate the electrochemical behavior of sophoridine at the GNPs/L-cys/rGO/GCE.

RESULTS AND DISCUSSION

Morphological characterization of the modified electrode

To obtain more information on the successful preparation of GNPs/L-cys/rGO/GCE, morphologies of different electrode were characterized by using SEM. The SEM images were randomly captured at different locations of the electrode surface. Fig. 3 shows typical SEM images of rGO/GCE (A), L-cys/rGO/GCE (B) and GNPs/L-cys/rGO/GCE (C), respectively. As showed in Fig. 3A, the films of rGO was typically thin, crumpled and displayed the edges of individual sheets. From Fig. 3B, it is clear that the films of L-cys has a regular growth and silkworm-like structure, and adhere on the surface of the film of rGO. According to our comparing experimental results, L-cys can be also electrodeposited onto the bare GCE, but regular growth of L-cys did not rise. Therefore, we suggest that the rGO film can induce the regular growth of L-cys. Fig. 3C is the image of the final composite employed in the present work. Fig. 3D is the energy-dispersive X-ray spectrum for the final composite which shows the following elements: C from graphene and L-cys; Au from GNPs and O from L-cysteine, suggesting GNPs can be allowed to self-assemble onto the regular growth of L-cys films. This result also indicated that combining GNPs with rGO via L-cys was successfully modified on the GCE just as designed.

Electrochemical characterization of the modified electrode

Electrochemical impedance spectroscopy (EIS) is an effective method of probing the interfacial properties of surface-modified electrodes. Fig. 4 shows the Nyquist diagrams of $[Fe(CN)_6]^{3-/4-}$ at bare GCE (curve a), rGO/GCE (curve b), L-cys/rGO/GCE (curve c) and GNPs/L-cys/rGO/GCE (curve d) in 5.0×10^{-3} mol L^{-1} K$_3$[Fe(CN)$_6$]/K$_4$[Fe(CN)$_6$] (1:1) containing 0.1 mol L^{-1} KCl solution. Obviously, all Nyquist plot had two parts (linear segment and semicircle part). Linear segment at lower frequencies
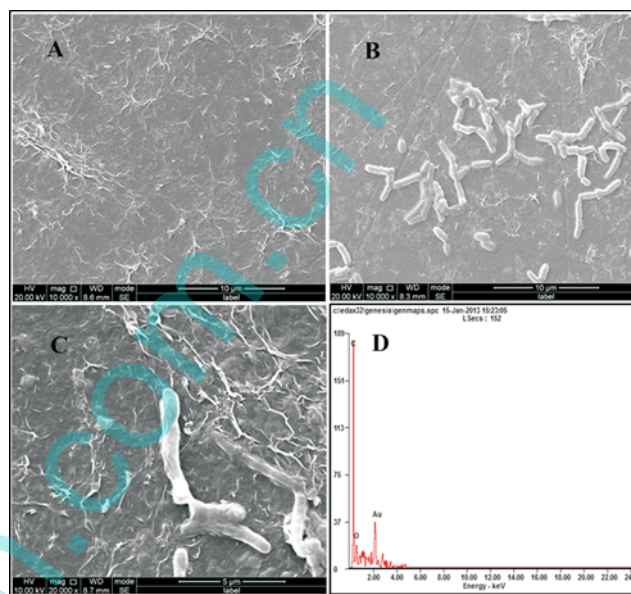

Fig. 3. SEM images of rGO/GCE (A), L-cys/rGO/GCE (B), GNPs/L-cys/rGO/GCE (C) and energy-dispersive X-ray spectrum for GNPs/L-cys/rGO/GCE (D).
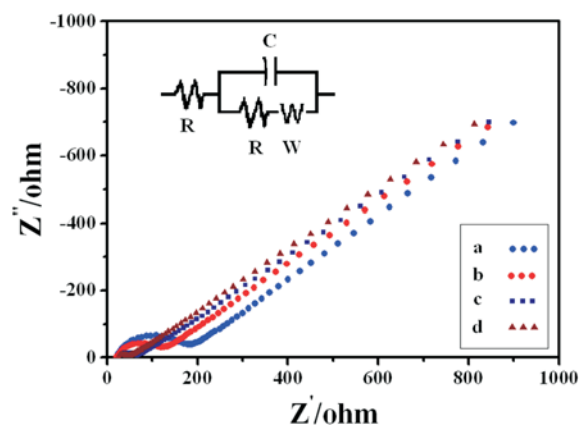

Fig. 4. EIS of a clean, freshly polished bare GCE (curve a), rGO/GCE (curve b), L-cys/rGO/GCE (curve c) and GNPs/L-cys/rGO/GCE (curve d) in a 5.0×10^{-3} mol L^{-1} Fe(CN)$_6$$^{4-/3-}$ (1:1) solution containing 0.10 mol L^{-1} KCl; open-circuit potential and amplitude of 5 mV; frequency range, 100000 Hz to 0.01 Hz; the inset is the equivalent circuit.

shows a controlled diffusion process;[27] and the semicircle part at higher frequencies corresponds to the electron transfer limited process or the electron transfer resistance (R_{ct}).[28] An equivalent circuit as showed in the insert of Fig. 4 was designed, and R_{ct} was obtained. The R_{ct} of the bare GCE was 135 Ω, which was larger than the R_{ct} of rGO/GCE (84 Ω), indicating that rGO film can improve the conductivity and the electron transfer process. With the electrodeposition of L-cys attached to the surface, the R_{ct} decreased further to 35 Ω, implying that the modification of L-cys film was more facile to the electron transfer. After nano-Au self-assembled monolayer being modified, it was clear that R_{ct} decreased to 21 Ω, demonstrating GNPs was successfully modified on the GCE just as designed. The reason may be that the GNPs immobilized on the electrode play an important role like a conducting wire or electron conduction tunnel, which makes it easier for the electron transfer to take place.

Voltammetric behavior of sophoridine at GNPs/L-cys/rGO/GCE

Fig. 5 displays cycle voltammograms (CVs) of 1.0×10^{-4} mol L^{-1} sophoridine in 0.2 mol L^{-1} PBS (pH 7.5) at the bare GCE (curve a), rGO/GCE (curve b), L-cys/rGO/GCE (curve c) and GNPs/L-cys/rGO/GCE (curve d), respectively. As can be seen, sophoridine showed electrochemical activation on all electrodes. At bare GCE, electrochemical response of sophoridine was very weak and only a very small bulge was observed. In contrast, on the rGO/GCE or L-cys/rGO/GCE, the oxidation peak cureents (i_{pa}) increased significantly and the peak potentials (E_p) was negatively shifted, indicating that the rGO and L-cys films could accelerated the electron transfer on the electrode surface to amplify the electrochemical signal due to its large surface area and excellent electric conductivity. When the GNPs/L-cys/rGO/GCE was applied, the most well-defined and sensitive anodic peak appeared under the same experimental condition, of which the i_{pa} is about 12.8, 1.51 and 1.34 fold higher than that of bare GCE, rGO/GCE and L-cys/rGO/GCE, respectively, and the E_{pa} is the lowest. This result testified that the use of GNPs as a modifier can facilitate the electron transfer between sophoridine and electrode. Besides, it also revealed that combining GNPs with rGO via L-cys can provide a more efficient interface and microenvironment for the electrochemical response of sophoridine. At the same time, the CVs of sophoridine exhibited only one anodic peak, with no peak on the reverse scan, indicating the electrode reaction was totally irreversible.

For further investigating the electrochemical properities of sophoridine at GNPs/L-cys/rGO/GCE, successive CVs were performed. The inset of Fig. 5 shows CVs of the background (curve a) and successive CVs of 1.0×10^{-4} mol L^{-1} sophoridine in 0.2 mol L^{-1} PBS (pH 7.5) at GNPs/L-cys/rGO/GCE (curve b). It is clear that the well-defined anodic peak is observed at the first cycle and decreased successively in following cycles. It resulted from the fact that the electrode surface was blocked by the adsorbed oxidation products which reduced the effective reaction sites at the modified electrode surface. Fortunately, we found that if the electrodes were kept in PBS (pH 7.5) in the absence of sophoridine for 3 min under constant stirring, and then CV was carried out in the solution with scan potential window of between 0.0 V to 1.0 V (vs SCE), until the peaks of sophoridine disappeared. Finally, the GNPs/L-cys/rGO/GCE surface will be restored to the initial state so that a new voltammogram then exhibits the same characteristics as those of the first cycle in the Fig. 5. Thus, the oxidation peak current in the first anodic sweep was used in following studies.

The effect of scan rate (v) on the oxidation of sophoridine has been studied by CV at GNPs/L-cys/rGO/GCE in differernt sweep rates from 50 to 300 mV s^{-1}, seen in Fig. 6. I_{pa} grows with the increasing of v and there are good linear relationships between i_{pa} and v, indicating that the anodic process of sophoridine taking place at the com-
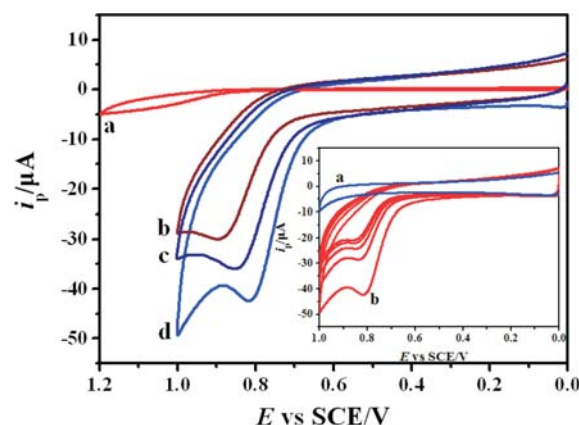

Fig. 5. CVs of 1.0×10^{-4} mol L^{-1} sophoridine at a bare GCE (curve a), rGO/GCE (curve b), L-cys/rGO/GCE (curve c) and GNPs/L-cys/rGO/GCE (curve d) in 0.2 mol L^{-1} PBS (pH = 7.5), v = 0.05 V s^{-1}; CVs of the background (curve a) and successive CVs of 1.0×10^{-4} mol L^{-1} sophoridine (curve b) at the GNPs/L-cys/rGO/GCE in the inset.
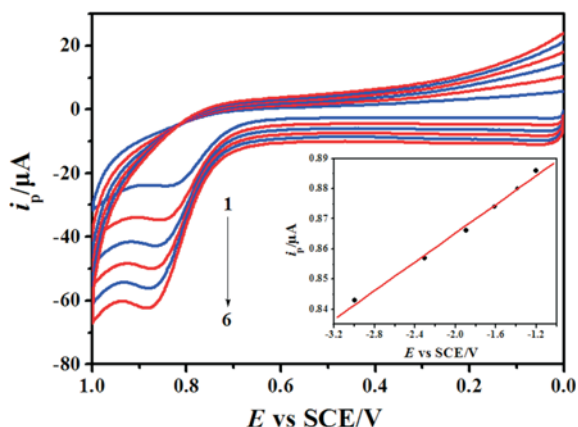
Fig. 6. CVs of 1.0×10^{-4} mol L^{-1} sophoridine at the GNPs/L-cys/rGO/GCE at different scan rate (from 1 to 6: 0.05, 0.10, 0.15, 0.20, 0.25, 0.30 V s^{-1}); insets show the relationship of the peak potential E_{pa} against ln v.

posite electrode is adsorption-controlled. Also, the oxidation peak potentials (E_{pa}) shift positively with the increasing of v. According to Laviron's theory,[29] for an irreversible anodic reaction, the relationship between E_{pa} and v is described as follows:

$$E_{pa}(V) = E^{\circ} - \frac{RT}{\alpha nF} \ln \frac{RTk_s}{\alpha nF} + \frac{RT}{\alpha nF} \ln v$$

where E° is the formal standard potential; α is the charge transfer coefficient; k_s is the apparent electron transfer rate constant; and others have their usual meaning. The inserted calibration plot in Fig. 6 highlight a linear relationship between the variation of E_{pa} with the v from 50 to 300 mV s^{-1} and a good linear equation was represented as E_{pa} (V) = $0.912 + 0.0238 \ln v$ (mV s^{-1}) ($R = 0.999$). From the slope of the straight line of E_{pa} against ln v, $\alpha n = 1.08$ could be obtained. The value of α can be calculated as:[29] $E_p - E_{p/2} = 1.857 (RT/\alpha F)$; where $E_{p/2}$ is the potential when the current is at the half peak value. From this, we obtained the value of α to be 0.61. Therefore, n was calculated to be 2. Meanwhile, the value of k_s of 1.65 s^{-1} was also calculated from the intercept of the straight line of E_{pa} vs. ln v. The value of E° was determined to be 0.835 V from intercept of E_{pa} versus v plot on the ordinate by extrapolating the line to be $v = 0$.

Chronocoulometry investigations

Chronocoulometry (CC) was used to characterize the oxidation of 5.0×10^{-4} mol L^{-1} sophoridine at GNPs/L-cys/rGO/GCE (Fig. 7). After the subtraction of the background charge, the plot of charges (Q) against $t^{1/2}$ has a linear rela-

tionship for the oxidation reaction for GNPs/L-cys/rGO/GCE (the inset of Fig. 7). According to the formula given by Anson:[30]

$$Q = \frac{2nFAc(Dt)^{1/2}}{\pi^{1/2}} + Q_{dl} + Q_{ads}$$

where c is the concentration of sophoridine, D is the diffusion coefficient, Q_{dl} is double-layer charge which could be eliminated by background subtraction, Q_{ads} is the Faradaic charge due to the oxidation of adsorbed sophoridine. Other symbols have their conventional meanings. It is clear that Q_{ads} can be obtained by differentiating the intercepts of the plots of Q versus $t^{1/2}$ in the presence and the absence of sophoridine (the inset of Fig. 7, curves a and b). According the equation $Q_{ads} = nFA\Gamma$, the values of the surface concentration (Γ) of sophoridine are 3.3×10^{-9} mol cm^{-2} at GNPs/L-cys/rGO/GCE.

Optimization of the analytical conditions

The types of supporting electrolytes played a key role in the voltammetric responses of sophoridine. Various buffers such as acetarte, borate, Britton Robinson, citrate and phosphate buffer were used. The best results with respect to sensitivity accompanied with sharper response were obtained with phoshate buffer (PBS). And then, studies were made in the pH range of 5.0~8.5 in PBS at a target concentration of 1.0×10^{-4} mol L^{-1} sophoridine solution. The results showed that the E_{pa} shifted to lower values as the pH increased. The relationship between the E_{pa} and pH could be fitted into the regression equation: E_{pa}(V) =
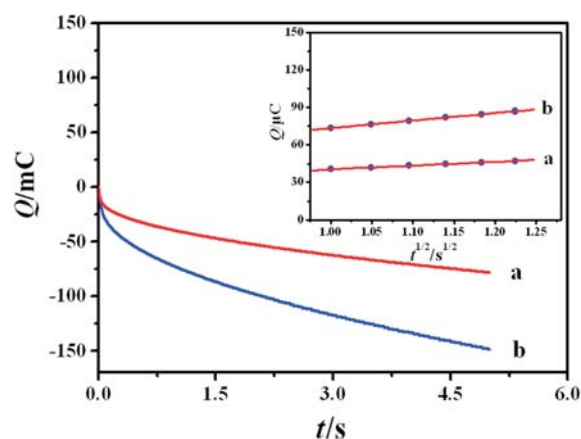

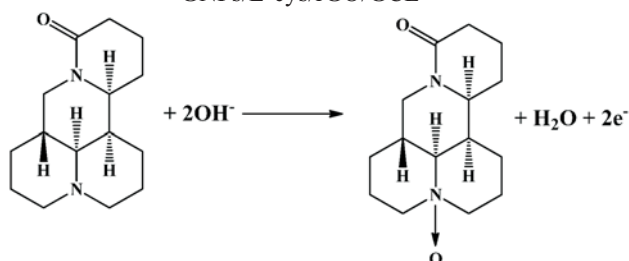Fig. 7. Chronocoulometric curves of the background (curve a) and 5.0×10^{-4} mol L^{-1} sophoridine (curve b) in 0.2 mol L^{-1} PBS (pH = 7.5) at the GNPs/L-cys/rGO/GCE; the inset is the corresponding $Q \sim t^{1/2}$ plots.

1.187–0.054 pH ($R = 0.998$), whose slope indicates that the same amounts of electrons and protons took part in the electrode reaction. Therefore, the oxidation mechanism for sophoridine can be written as Scheme 2, which is in accordance with the report.[15,16] Besides, the i_{pa} vary very little in the range of 7.0~7.5; so solution pH of 7.5 was chosen in following experiments, which was close to human physiological pH.

Scheme 2 Oxidation mechanism of sophoridine at GNPs/L-cys/rGO/GCE

Accumulation conditions

For an adsorbed-driven electrode reaction, it is good ways for enhancing the detect sensitivity by preconcentration. In the experiments, the influence of the accumulation time (t_{acc}) on response currents of 2.0×10^{-5} mol L^{-1} sophoridine was estimated. The results showed that the i_{pa} increased greatly within 240 s and then enhanced slowly. It is well-known that a longer t_{acc} will result in a better detection limit, but will also lead to a narrower linear range. For comprehensive consideration, 240 s was chosen as accumulation time. Moreover, the accumulation potential had little effect on the i_{pa}. So the accumulation was carried out under an open circuit.

Calibration curve, detection limit, repeatability and stability

Series concentrations of sophoridine standard solutions were detected under the optimized working conditions described above. Fig. 8 displays the response of different concentration of sophoridine by differential pulse adsorptive stripping voltammetry (DPASV). A linear relationship could be established between i_{pa} and the concentration of sophoridine in the range of 1.0×10^{-6}~1.0×10^{-4} mol L^{-1}. The linear regression equation and correlation coefficient are:

$$i_{pa} = 4.268 + 0.244\,c \quad (R = 0.999)$$

where i_{pa} was the oxidation peak current in μA and c was

the concentration of sophoridine in μmol L^{-1}. Standard deviations (SD) for the slope and intercept of the calibration curve were 0.00578 and 0.0278, respectively. Based on the signal-to-noise ratio of 3 (S/N),[31] the detection limit was obtained as 4.0×10^{-7} mol L^{-1}. These values confirmed the sensitivity of the proposed method of the determination of sophoridine.

To estimate the repeatability of the proposed electrode, the R.S.D. of five times successful measurement the peak current of 2.0×10^{-5} mol L^{-1} sophoridine was calculated to be 3.9%, which demonstrated the good repeatability of the proposed electrode. The GNPS/L-cys/rGO/GCE can be stored about 1 weeks and the decrease of the response was got as 3.7%, which indicated that GNPS/L-cys/rGO/GCE had good stability.

The proposed GNPS/L-cys/rGO/GCE for sophoridine determination was compared with other method reported and the results were listed in Table 1. The GNPS/L-cys/rGO/GCE showed good sensitivity with a detection limit of 4.0×10^{-7}. This result suggests that the modified electrode as voltammetric sensors might be a very promising direction in trace analysis of electrochemistry.

Interference studies

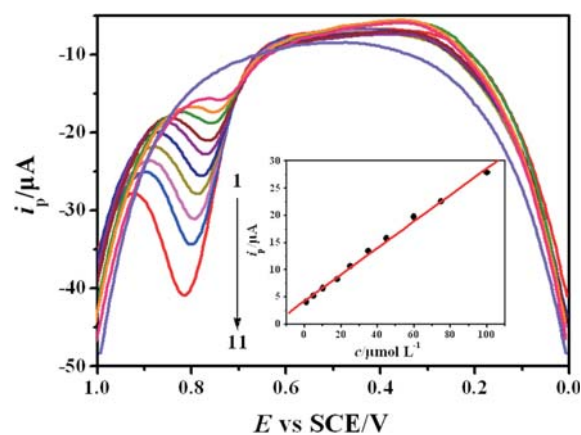The influence of various potentially interfering sub-

Fig. 8. Differential pulse adsorptive stripping voltammograms and their associated calibration plot (insert) for increasing concentrations of sophoridine at the GNPs/L-cys/rGO/GCE under optimum conditions, following accumulation: t_{acc} = 210s and open circuit; sophoridine concentration: (1) 0.0 mol L^{-1}, (2) 1.0×10^{-6} mol L^{-1}, (3) 5.0×10^{-6} mol L^{-1}, (4) 1.0×10^{-5} mol L^{-1}, (5) 1.8×10^{-5} mol L^{-1}, (6) 2.5×10^{-5} mol L^{-1}, (7) 3.5×10^{-5} mol L^{-1}, (8) 4.5×10^{-5} mol L^{-1}, (9) 6.0×10^{-5} mol L^{-1}, (10) 7.5×10^{-5} mol L^{-1}, (11) 1.0×10^{-4} mol L^{-1}.

Table 1. Comparison of determination of sophoridine by different sensing methods reported

Modifier	Methods	Linear range	Detection limit (mol L^{-1})	Reference
Poly (L-Theanine)	Amperometric detection	$1.0 \times 10^{-6} \sim 1.4 \times 10^{-4}$	5.0×10^{-7}	15
ERGO	SWASV	$8.0 \times 10^{-7} \sim 1.0 \times 10^{-4}$	2.0×10^{-7}	16
GNPs/L-cys/rGO/GCE	DPASV	$1.0 \times 10^{-6} \sim 1.0 \times 10^{-4}$	4.0×10^{-7}	This work

SWASV: square wave adsorptive stripping voltammetry.
DPASV: differential pulse anodic stripping voltammetry.

Table 2. Application of the DPASV method to the determination of sophoridine in injection samples

DPASV (n = 5)						UV (n = 3)	
Declared content (mol L^{-1})	Amount found (mol L^{-1})	RSD (%)	Standard added (mol L^{-1})	Total found/ (mol L^{-1})	Recovery (%)	Amount found (mol L^{-1})	RSD (%)
5.00×10^{-2}	5.24×10^{-2}	2.7	2.50×10^{-2}	7.68×10^{-2}	97.6	5.30×10^{-2}	0.29

stances for determination of 5.0×10^{-5} mol L^{-1} sophoridine was studied. The results indicated that 100-fold of Ca^{2+}, Zn^{2+}, Cu^{2+}, Cl^{-}, SO$_4^{2-}$, NO$_3^{-}$, Ac^{-}, glucose, sucrose and amylum, 10-fold of hypoxanthine, glycine, glutamic acid, ascorbic acid, uric acid, epinephrine, adenine had almost no influence on the determination and the tolerance limit was estimated to be less than 5% of the relative error, indicating the present method was adequate for the determination of sophoridine in real samples.

Determination of sophoridine in injection samples

In order to evaluate the validity of the proposed method, it was employed to determine sophoridine in injection samples. The sample was diluted with the supporting electrolyte to operate in the linear range of the method and to reduce the matrix effect. After the content of sophoridine was evaluated, a standard sophoridine solution was added to the sample and the total content of sophoridine was determined to calculate the recovery (see Table 2). For testing the accuracy of the proposed method, the same samples were analyzed using UV-vis method and the results were listed in Table 1 too. The contents obtained from the proposed method and UV-vis method were compared using *t*-test under 95% confidence levels. The results proved that there is no significant difference between them. The results showed that the method was reliable for the quantitative determination of sophoridine in injection samples.

CONCLUSIONS

In sum, we have successfully fabricated a new electrochemical sensor through combining gold nanoparticles (GNPs) with reduced graphene oxide (rGO) via L-cysteine (L-cys) as crosslinker. The resulting electrode was applied to develop a high-sensitive electrochemical sensor for determination of sophoridine. Wide linear concentration ranges, low detection limits, and excellent repeatability and stability were achieved on the modified electrode, indicating the proposed method might be a very promising platform for analytical sensing.

REFERENCES

1. Zhao, B. G. *Acta Pharm. Sin.* **1980**, *15*, 182.
2. Liu, T. H.; Liu, D. F.; Wang, J.; *et al. Acad. J. Second Military Med. Univ.* **2010**, *31*, 399.
3. Liu, T. H.; Liu, D. F.; Wang, J.; *et al. Chin. J. Inf. Tradit. Chin. Med.* **2010**, *17*, 31.
4. Zhang, W. M.; Zhang, Y. M.; Zhang, T.; *et al. Prog. Vet. Med.* **2005**, *26*, 82.
5. Zhou, Y.; Wang, N. P.; Zhao, J. N.; *et al. Liaoning J. Tradit. Chin. Med.* **2000**, *27*, 84.
6. Liang, L.; Zhang, X. H.; Wang, X. Y.; *et al. Zhongguo Yaolixue Tongbao* **2008**, *24*, 782.
7. Li, X. M.; Wu, Y. G.; Pan, D. X.; *et al. Chin. J. New Drugs* **2006**, *15*, 654.
8. Yang, Z. W.; Zhou, Y.; Cao, X. Q. *Sichuan J. Tradit. Chin. Med.* **2003**, *21*, 14.
9. Nie, H. M.; Chen, J. J.; Gao, Y. Q.; *et al. Beijing J. Tradit. Chin. Med.* **2007**, *26*, 678.
10. Wei, Y. H.; Wu, X. A.; Liu, X. F.; *et al. J. Chromatogr., B* **2006**, *843*, 10.

11. Wu, Y. J.; Chen, J. J.; Cheng, Y. Y. *Anal. Bioanal. Chem.* **2005**, *382*, 1595.

12. Chen, N.; Han, Z.; Luan, L.; *et al. Chromatographia* **2009**, *70*, 299.

13. Song, J. Z.; Xu, H. X.; Tian, S. J.; *et al. J. Chromatogr., A* **1999**, *857*, 303.

14. Chen, X.; Yi, C. Q.; Li, M. J.; *et al. Anal. Chim. Acta* **2002**, *466*, 79.

15. Li, Y. F.; Zou, L. N.; Song, G.; *et al. J. Electroanal. Chem.* **2013**, *709*, 1.

16. Wang, F.; Wu, Y.; Lu, K.; *et al. Electrochim. Acta* **2014**, *141*, 82.

17. Zhou, M.; Ding, J.; Guo, L. P.; *et al. Anal. Chem.* **2007**, *79*, 5328.

18. Banks, C. E.; Davies, T. J.; Wildgoose, G. G.; *et al. Chem. Commun.* **2005**, 829.

19. Wang, F.; Wang, Y. W.; Lu, K.; *et al. J. Electroanal. Chem.* **2012**, *674*, 83.

20. Geim, A. K. *Science* **2009**, *324*, 1530.

21. Geim, A. K.; Novoselov, K. S. *Nat. Mater.* **2007**, *6*, 183.

22. Zhang, J. L.; Yang, H. J.; Shen, G. X.; *et al. Chem. Commun.* **2010**, *46*, 1112.

23. Arvand, M.; Gholizadeh, T. M. *Sens. Actuators, B* **2013**, *186*, 622.

24. Sanghavi, B. J.; Kalambate, P. K.; Karna, S. P.; *et al. Talanta* **2014**, *120*, 1.

25. Tsutsui, G.; Huang, S.; Sakaue, H.; *et al. Jpn. J. Appl. Phys., Part 1* **2001**, *40*, 346.

26. Hummers, W. S.; Offeman, R. E. *J. Am. Chem. Soc.* **1958**, *80*, 1339.

27. Liu, Y.; Yin, F.; Long, Y.; *et al. J. Colloid Interface Sci.* **2003**, *258*, 75.

28. Pei, R.; Cheng, Z.; Wang, E.; *et al. Biosens. Bioelectron.* **2001**, *16*, 355.

29. Laviron, E. *J. Electroanal. Chem.* **1979**, *101*, 19.

30. Anson, F. C. *Anal. Chem.* **1964**, *36*, 932.

31. Miller, J. N.; Miller, J. C. *Statistics and Chemometrics for Analytical Chemistry*, 4th ed.; Pearson Education Limited: London, 2000.